Mathematical Modeling of the Argon-Oxygen Decarburization Refining Process of Stainless Steel: Part I. Mathematical Model of the Process

JI-HE WEI and DE-PING ZHU

Some available mathematical models for the argon-oxygen decarburization (AOD) stainless steel–making process have been reviewed. The actual situations of the AOD process, including the competitive oxidation of the elements dissolved in the molten steel and the changes in the bath composition, as well as the nonisothermal nature of the process, have been analyzed. A new mathematical model for the AOD refining process of stainless steel has been proposed and developed. The model is based on the assumption that the blown oxygen oxidizes C, Cr, Si, and Mn in the steel and Fe as a matrix, but the FeO formed is also an oxidant of C, Cr, Si, and Mn in the steel. All the possible oxidation-reduction reactions take place simultaneously and reach a combined equilibrium in competition at the liquid/bubble interfaces. It is also assumed that at high carbon levels, the oxidation rates of elements are primarily related to the supplied oxygen rate, and at low carbon levels, the rate of decarburization is mainly determined by the mass transfer of carbon from the molten steel bulk to the reaction interfaces. It is further assumed that the nonreacting oxygen blown into the bath does not accumulate in the liquid steel and will escape from the bath into the exhaust gas. The model performs the rate calculations of the refining process and the mass and heat balances of the system. Also, the effects of the operating factors, including adding the slag materials, crop ends, and scrap, and alloy agents; the nonisothermal conditions; the changes in the amounts of metal and slag during the refining; and other factors have all been taken into account.

I. INTRODUCTION

THE keys for the refining of stainless steel are how to remove effectively the carbon in the steel and to raise the chromium recovery. In the various refining technologies of stainless steel, the argon-oxygen decarburization (AOD) process has a number of obvious advantages; thus, it has been applied extensively and developed rapidly throughout the world. At present, over 75 pct of the world's stainless steel output is produced using the process.

Simultaneously, many studies on mathematical modeling for the AOD refining of stainless steel have been carried out, and numerous models have been proposed and developed to attempt to accomplish optimization and computer control of the process.[1–11] Taking the AOD refining of low-carbon and high-chromium stainless steel as an example, Ray and Szekely[1] examined and analyzed the mathematical modeling of this process in the discussion of process optimization methods. Following this work, based on the mass and heat balances of the system and the film theory of diffusion, Asai and Szekely[2,3] proposed a mathematical model for the decarburization of stainless steel. The essential assumption was that the oxygen supplied to the metal is either used to participate selectively in decarburization and the oxidative reactions of Cr and Si, thus forming CO, Cr_2O_3, and SiO_2, or it accumulates in the metal phase. The model did not allow for the formation of FeO explicitly; namely, it postulated that the oxygen transfer from the FeO part of the slag to the metal is quite rapid. Applying the model to the refining process in an oxygen-blown, electric furnace of 40-t capacity, the predictions and measurements showed quite good agreement. The first deficiency of this model is that the discrepancy of decarburization patterns at high and low carbon levels was not noted. Second, according to this model, the rate parameters used were the conductances determined by consider all the resistances of the system to transfer, *i.e.*, mass transfer, chemical kinetics, mixing, *etc.* So, the values of these conductance parameters for different components in the bath must be different under different operating conditions. However, it was assumed that the values of these parameters for the overall transfer of C, O, Cr, and Si under different operating modes were equal and constant. These assumptions, combined with the assumption that all nonreacting oxygen is accumulated in the molten stainless steel, are in clear contradiction to known phenomena and likely to lead to errors in predicting the kinetics of the AOD processes.

Fruehan[4] assumed that most of the oxygen blown is consumed in the oxidation of chromium in the tuyere zone, and the Cr_2O_3 formed oxidizes the carbon as it rises in the bath with the argon bubbles (FeO may also form, but it is quickly reduced by Cr). It was further assumed that the oxidation of carbon by Cr_2O_3 is controlled by the liquid-phase mass transfer of carbon to the bubble surface at low carbon levels and is determined primarily by the rate of oxygen blown at high carbon levels. Also, it was assumed that most of the silicon is preferentially oxidized to the chromium in the early stage of the blow. On the basis of these assumptions, a reaction model was developed to predict the rates of carbon and chromium oxidation in the AOD process. It has been confirmed by numerous observations

JI-HE WEI, Professor, is with the Department of Metallic Materials, Shanghai University, Shanghai, 200072, People's Republic of China. DE-PING ZHU, formerly Graduate Student, Department of Metallic Materials, Shanghai University, is Engineer, Shanghai Wensi Sorftware Limited Company.

Manuscript submitted January 9, 2001.

of pneumatic steelmaking processes, including the converter and AOD processes, that there exist distinct regimes of rate control for decarburization at high and low carbon levels. However, the oxygen blown into the bath during the refining process cannot usually be completely absorbed.[12] The assumptions of complete utilization of oxygen, of a reaction scheme, and of isothermal conditions are potential sources of weakness in the model developed by Fruehan.

Deb Rey and Robertson[5,6] considered that all the injected oxygen oxidizes the chromium, silicon, and manganese dissolved in the liquid steel, and the Cr_2O_3, SiO_2, and MnO formed are reduced by carbon as they rise in the bath with the bubbles. Moreover, they noted the change in the partial pressure of carbon monoxide with the bath height and introduced the heat balance to take account into the nonisothermal nature of the bath, thus, proposing a mathematical model for stainless steel making. The model was tested on plant data obtained in producing Type 304 stainless steel in a 45-t AOD converter, and better results were obtained. However, the fact that there are different decarburization patterns at high and low carbon contents was also not reflected by the model. Furthermore, they assumed that the oxygen distribution ratios near the jet entrance among the dissolved elements were proportional to the molar concentrations of the elements. This assumption and the assumption of complete oxygen utilization are potential sources of error in this model.

Ohno and Nishida[7] proposed a bubble decarburization model for the AOD process. They also assumed that the injected oxygen primarily oxidizes chromium in the tuyere zone and that the chromium oxide formed subsequently oxidizes the carbon as it rises in the bath with the argon bubbles. At the same time, they assumed that the reductive reaction of Cr_2O_3 by carbon is, all along, limited by the liquid-phase mass transfer of carbon to the bubble surface in the whole refining process. Considering the influence of the bath height on the total pressure and partial pressure of CO in the bubble, the rate equation of the decarburization process, characterized by the partial pressure of CO, was derived and obtained. As mentioned previously, it is not likely that the mass transfer of carbon becomes a limiting link of the rate of the decarburization process at high carbon levels. In addition, the effects of the operating factors and changes in the bath composition and temperature in the refining process were not considered. The activities of the elements in the steel were taken to be all 1, which must also bring about a considerable deviation from reality.

Tohge *et al.*[8] investigated experimentally the refining process of austenitic-grade stainless steel with very a high initial content of carbon (>2.5 mass pct) in a top-and-bottom-combined blowing AOD vessel of 70-t capacity using the operating practice of a high gas bottom blowing rate with oxygen top blowing. On the basis of the mass and heat balances, they developed a theoretical model which considered the formation of some amount of FeO, nonisothermal conditions, and rate-controlling steps, as well as the addition of slag, scrap, and alloy agents. According to their model, the carbon, silicon, chromium, manganese, and iron in the steel are oxidized during the oxidation in the AOD process, thus forming CO, SiO_2, Cr_2O_3, MnO, and FeO. It should be said that the conditions of the AOD refining were, throughout, of quite concern in this model. However, it must again be pointed out that the assumption of the rate-controlling steps all being the liquid-phase mass transfer, in the cases of high and low carbon levels, is not reasonable. Additionally, the diluting role of the inert gas blown to the carbon monoxide formed and its effect on the rate of decarburization were not fully reflected. Also, it is not likely that the oxygen in the gas blown through the tuyeres from the vessel bottom is completely consumed by the oxidation of the various elements in the steel. The estimation of a Gibbs free energy for the reaction of $1/3\langle Cr_2O_3\rangle + [Fe] = (FeO) + 2/3[Cr]$ indicated that there is no possibility of the oxidation of iron in terms of the reaction, even under their experimental conditions (the corresponding equilibrium constant at 1700 °C is about 0.0245). So, this assumption regarding the oxidation of iron cannot be held.

Using similar assumptions to those of Fruehan's model, a mathematical model for the AOD refining process of stainless steel was developed by Reichel and Szekely.[9] According to this model, the decarburization rate is proportional to the supplied oxygen rate at high carbon levels and is related to the carbon content and the supplied oxygen rate at low carbon levels, but the influence of the latter weakens. A critical state or a critical point exists in the refining process, when the constant rate of decarburization transitions to a falling rate. The corresponding carbon concentration is the critical carbon content. Essentially, this model has the same weaknesses as those of Fruehan's model.

In terms of the thermodynamics with the mass balance of the system, Görnerup and Sjöberg[10] mathematically modeled the AOD/Creusot–Loire Uddeholm process. The principal question to their model is that the state of thermodynamic equilibrium, in fact, cannot be reached and established in the whole bath during the refining process. So, it is hard to say that their model is reliable and believable. Recently, taking the rate equation of Fruehan's model at the low-carbon condition and the heat balance of the system as a basis, a real-time online control model for the AOD process was developed.[11] The results, applied to the refining process in a 68-t AOD vessel, indicated that the calculation and control precision of this model are not high.

To sum up, these studies, to different extents, offered some useful information for understanding and improving the process practice. However, all these available models have not reflected and described fully the real situations of the refining process of stainless steel and, to a certain degree, have all those shortcomings. Using these models, in fact, it is difficult to predict quantitatively and accurately the changes in the chemical composition and temperature of the bath during the practical process and the influence of the relevant factors, as well as their interactions. It is still needed, and is of important theoretical and practical meaning, to study further and more deeply this process. Considering these conditions, the AOD refining of stainless steel has been investigated. A new mathematical model for this process has been proposed and developed, which is expect to provide more believable and useful information and a more reliable basis for the optimization and computer control of the process. The model performs the rate calculations of the refining process and the mass and heat balances of the system. Simultaneously, the effects of the operating factors, including adding the slag materials, crop ends, and scrap, and alloy agents; the nonisothermal conditions; the changes in the amounts

of slag and metal during the refining; and other factors were all considered. The details of the model and the determination of its parameters with the computing procedure are presented in Part I of the present work.

II. ANALYSIS OF THE AOD PROCESS

It is well known that in AOD stainless steel making, the supplied oxygen is utilized to remove the carbon in the molten steel. The argon (or nitrogen) blown simultaneously can decrease the partial pressure of the carbon monoxide and promote decarborization, thus achieving the effectiveness and objective of removing carbon and reducing the loss of chromium. However, the silicon and manganese dissolved in the molten steel can also absorb the blown oxygen and restrict the oxidation reactions of carbon and chromium. Due to their low initial contents in the steel, their oxidative reactions during the refining process will rapidly reach the relevant dynamic equilibrium. After that, the supplied oxygen will, apparently, all be consumed by the oxidation of carbon and chromium, except the part escaped from the bath. That is to say, there exists throughout the competitive oxidation of the carbon, chromium, silicon, manganese, and other elements dissolved in the steel during the whole refining process.

Moreover, at high carbon concentrations, the driving force for the mass transfer of carbon in the liquid steel to the reaction interface would be high enough at the oxygen blow rates usually used in the AOD practice. In this case, there would be insufficient oxygen to oxidize the carbon transferred to the reaction interface from the bulk of the molten steel. This means that at high carbon concentrations, the rate of decarburization would primarily be related to the rate of oxygen blow. When the carbon content in the steel is decreased to a certain low level, the rate of decarburization may change to being controlled by the mass transfer of carbon to the reaction interface from the liquid bulk. Numerous observations of the AOD refining process suggest that there is a critical point or a critical state in the process like that in oxygen-converter steelmaking. This point corresponds to the critical carbon concentration and to the transition from the decarburization rate being related to the supplied oxygen amount to being the rate controlled by the mass transfer of carbon in the liquid phase.

The oxygen molecules entering the bath would also contact the iron atoms as a matrix of stainless steel and form iron oxide, but most of the iron oxide formed would, subsequently, quickly be reduced by the carbon, chromium, silicon, manganese and other elements in the molten steel. This means that the iron oxide formed also would be an oxidant for them and would be mainly an intermediate product of the gas-blowing refining. In addition, their oxidation, to a certain extent, would be related to the supplied oxygen rate even at low carbon concentration levels.

Furthermore, the bath always demonstrates an obvious nonisothermal characteristic during the refining process. The oxidation reactions of the elements dissolved in the steel make the bath temperature continuously increase; the addition of slag materials, crop ends, scrap, and alloy agents, as well as the heat loss of the system, cools the bath. The nonisothermal nature of the bath can directly and strongly influence the equilibrium and rates of the various refining reactions.

Another feature of the AOD process is that the bath is strongly agitated by the gas streams. The fluids in the bath undergo very vigorous stirring and circulatory motion during gas blowing, and there is no obvious dead zone in the bath.[13] This can very effectively promote and intensify the heat and mass transfer and is undoubtedly very advantageous in accelerating the refining reactions and improving the homogeneity of the bath composition and temperature.

The conditions and characteristics mentioned previously must all be considered and noted in mathematical modeling of the AOD refining process of stainless steel.

III. MATHEMATICAL MODEL OF THE PROCESS

A. *Basic Assumptions of the Model*

In order to propose and develop a new mathematical model to deal with the refining process, the following initial assumptions were made for the process, based on the previous analysis.

(1) The oxygen blown into the molten steel simultaneously oxidizes the carbon, chromium, silicon, and manganese dissolved in the steel and the iron as a matrix; the iron oxide formed is also an oxidant for the other elements and is, essentially, an intermediate product of the refining process.
(2) All the possible oxidation-reduction reactions take place simultaneously and reach and establish a combined equilibrium in competition at the liquid/bubble interfaces.[14–18]
(3) At high carbon contents, the oxidation rates of elements are primarily related to the supplied oxygen rate; at low carbon concentration levels, the rate of decarburization is mainly determined by the mass transfer of carbon in molten steel.
(4) The unabsorbed oxygen blown into the liquid steel will escape from the bath and form CO_2 with CO in the exhaust gas, rather than dissolving and accumulating in the steel.
(5) The bath composition and temperature are continually changing and are uniformly distributed at any moment during the whole refining process.
(6) The oxidation of elements in the steel other than C, Cr, Si, and Mn is temporarily not taken into account; *i.e.*, the oxygen consumed by the other elements is ignored in the present work.

B. *Refining Reaction Schemes*

The oxidative reactions of the carbon, chromium, silicon, and manganese dissolved in the molten steel and the iron as a matrix of the steel by the blown oxygen can be written as

$$[C] + \frac{1}{2}O_2 = \{CO\} \quad [1]$$

$$2[Cr] + \frac{3}{2}O_2 = (Cr_2O_3) \quad [2]$$

$$[Si] + O_2 = (SiO_2) \quad [3]$$

$$[Mn] + \frac{1}{2}O_2 = (MnO) \quad [4]$$

$$[Fe] + \frac{1}{2}O_2 = (FeO) \quad [5]$$

The reaction system is just one composed of a liquid alloy (stainless steel) and a liquid slag phase with an atmosphere containing oxygen. The following independent reaction equilibria in this system can be produced from combinations of reactions [1] through [4], respectively, with reaction [5].

$$[C] + (FeO) = \{CO\} + [Fe]; \qquad \Delta G_C = \Delta G_C^\circ + RT \ln \frac{P_{CO}}{a_{[C]} a_{(FeO)}} \quad [6]$$

$$2[Cr] + 3(FeO) = (Cr_2O_3) + 3[Fe]; \qquad \Delta G_{Cr} = \Delta G_{Cr}^\circ + RT \ln \frac{a_{Cr_2O_3}}{a_{[Cr]}^2 a_{(FeO)}^3} \quad [7]$$

$$[Si] + 2(FeO) = (SiO_2) + 2[Fe]; \qquad \Delta G_{Si} = \Delta G_{Si}^\circ + RT \ln \frac{a_{(SiO_2)}}{a_{[Si]} a_{(FeO)}^2} \quad [8]$$

$$[Mn] + (FeO) = (MnO) + [Fe]; \qquad \Delta G_{Mn} = \Delta G_{Mn}^\circ + RT \ln \frac{a_{(MnO)}}{a_{[Mn]} a_{(FeO)}} \quad [9]$$

These all belong among the possible reactions which occur in the system. Thermodynamically, the reaction schemes presented by reactions [1] through [5] and reactions [6] through [9] can all characterize the chemical-equilibrium feature of the refining system but, kinetically, they are different, the former being direct, and the latter being indirect.

C. *Rate Equations of the Process*

At high carbon contents, the average loss rates of the carbon, chromium, silicon, and manganese dissolved in the steel in the competitive oxidation are, separately,

$$-\frac{W_m}{100\ M_C} \frac{d[\text{pct C}]}{dt} = \frac{2\eta Q_O}{22{,}400} x_C \quad [10]$$

$$-1.5 \frac{W_m}{100\ M_{Cr}} \frac{d[\text{pct Cr}]}{dt} = \frac{2\eta Q_O}{22{,}400} x_{Cr} \quad [11]$$

$$-2 \frac{W_m}{100\ M_{Si}} \frac{d[\text{pct Si}]}{dt} = \frac{2\eta Q_O}{22{,}400} x_{Si} \quad [12]$$

$$-\frac{W_m}{100\ M_{Mn}} \frac{d[\text{pct Mn}]}{dt} = \frac{2\eta Q_O}{22{,}400} x_{Mn} \quad [13]$$

At low carbon concentration levels, the average rate of decarburization can be expressed as

$$-W_m \frac{d[\text{pct C}]}{dt} = A_{rea} \rho_m k_C ([\text{pct C}] - [\text{pct C}]_e) \quad [14]$$

At this time, the refining reactions in the bath mainly are the oxidation of carbon and chromium, and the bath temperature is also raised to a higher level. Thus, the following reaction can appropriately be considered:

$$(Cr_2O_3) + 3[C] = 2[Cr] + 3\{CO\} \quad [15]$$

Correspondingly, the equilibrium concentration of carbon at the reaction interface is

$$[\text{pct C}]_e = \frac{P_{CO}}{f_C} \sqrt[3]{\frac{a_{[Cr]}^2}{a_{Cr_2O_3} K_{Cr-C}}} \quad [16]$$

where $a_{[Cr]} = f_{Cr}[\text{pct Cr}]$ and $a_{(Cr_2O_3)} = \gamma_{Cr_2O_3} N_{Cr_2O_3}$. Clearly, reaction [15] can be reached by a combination of reactions [1] and [2] or reactions [6] and [7]. Paying attention to the diluting role of the inert gas (argon or nitrogen) and nonreacting oxygen, the partial pressure of carbon monoxide (P_{CO}) should be

$$P_{CO} = \frac{n_{CO}}{n_{CO} + n'_O + n_{sub}} P_t$$

Relevantly,

$$n_{CO} = \frac{W_m}{100\ M_C} \left(-\frac{d[\text{pct C}]}{dt} \right) dt$$

and $n'_O = Q_O(1 - \eta)dt/22{,}400$ and $n_{sub} = Q_{sub}dt/22{,}400$. Thus, the following expression can be reached:

$$P_{CO} = \frac{-\frac{d[\text{pct C}]}{dt}}{\frac{100\ M_C}{W_m} \frac{Q_O(1 - \eta) + Q_{sub}}{22{,}400} - \frac{d[\text{pct C}]}{dt}} P_t \quad [17]$$

Substituting Eqs. [16] and [17] into Eq. [14], the following can be obtained:

$$\frac{d[\text{pct C}]}{dt} = \frac{1}{2} (-s_1 - \sqrt{s_1^2 + s_2}) \quad [18]$$

where

$$s_1 = -\frac{100\ M_C}{W_m} \frac{Q_O(1 - \eta) + Q_{sub}}{22{,}400} + \frac{A_{rea} \rho_m k_C}{W_m} \left(-\frac{P_t}{f_C} \sqrt[3]{\frac{a_{[Cr]}^2}{a_{Cr_2O_3} K_{Cr-C}}} + [\text{pct C}] \right) \quad [19]$$

$$s_2 = 4 \frac{A_{rea} \rho_m k_C}{W_m} [\text{pct C}] \left(\frac{100\ M_C}{W_m} \right) \frac{Q_O(1 - \eta) + Q_{sub}}{22{,}400} \quad [20]$$

D. *Heat Balance of the System*

The molten steel, slag melt, and gases (including the blown oxygen and argon (or nitrogen) and the exhaust gas) all carry heat. The oxidation reactions of elements can release heat. Also, the heat of the system can be lost by conduction and adsorption of the refractory lining and shell during the rising-temperature process of the bath; by radiation; by the operations of taking the samples and measuring the temperature; by adding the slag materials, crop ends, scrap, and alloy agents; and by other factors. Moreover, the heat can be obtained or lost due to some uncertain reasons. According to these, the heat-balance equation is

$$
\begin{aligned}
&W_m c_{p,m} T + Q_O dt \rho_O c_{p,O} T_{g,0} + Q_{sub}\, dt \rho_{sub} c_{p,sub} T_{g,0} + W_s c_{p,s} T \\
&\quad + \frac{W_m}{100}\left(-\frac{d[\text{pct C}]}{dt}\Delta H_C - \frac{d[\text{pct Cr}]}{dt}\Delta H_{Cr}\right. \\
&\quad \left. - \frac{d[\text{pct Mn}]}{dt}\Delta H_{Mn} - \frac{d[\text{pct Si}]}{dt}\Delta H_{Si}\right)dt \\
&\quad = W_m\left(1 + \left(\frac{d[\text{pct C}]}{dt} + \frac{d[\text{pct Cr}]}{dt} + \frac{d[\text{pct Mn}]}{dt}\right.\right. \\
&\quad \left.\left. + \frac{d[\text{pct Si}]}{dt}\right)\frac{dt}{100}\right)c_{p,m}(T + dT) \qquad [21] \\
&\quad + Q_O(1-\eta)dt\rho_O c_{p,O} T_g + Q_{sub} dt \rho_{sub} c_{p,sub} T_g \\
&\quad + \frac{W_m}{100}\left(-\frac{d[\text{pct C}]}{dt}\right)dt\frac{M_{CO}}{M_C}c_{p,CO} T_g \\
&\quad + \left(W_s - \frac{W_m dt}{100}\left(\frac{d[\text{pct Cr}]}{dt}\frac{M_{Cr_2O_3}}{2M_{Cr}}\right.\right. \\
&\quad \left.\left. + \frac{d[\text{pct Mn}]}{dt}\frac{M_{MnO}}{M_{Mn}} + \frac{d[\text{pct Si}]}{dt}\frac{M_{SiO_2}}{M_{Si}}\right)\right)c_{p,s}(T + dT) \\
&\quad + (q_{loss} + q_5)dt
\end{aligned}
$$

The appropriate rising rate of the bath temperature is

$$
\begin{aligned}
\frac{dT}{dt} &= \left(c_{p,s} T\left(\frac{M_{Cr_2O_3}}{2M_{Cr}}\frac{d[\text{pct Cr}]}{dt} + \frac{M_{MnO}}{M_{Mn}}\frac{d[\text{pct Mn}]}{dt}\right.\right. \\
&\quad \left. + \frac{M_{SiO_2}}{M_{Si}}\frac{d[\text{pct Si}]}{dt}\right) - c_{p,m} T\left(\frac{d[\text{pct C}]}{dt} + \frac{d[\text{pct Cr}]}{dt}\right. \\
&\quad \left. + \frac{d[\text{pct Mn}]}{dt} + \frac{d[\text{pct Si}]}{dt}\right) \\
&\quad - \frac{100}{W_m}(Q_O \rho_O c_{p,O}((1-\eta)T_g - T_{g,0}) \qquad [22] \\
&\quad + q_{loss} + q_5) + c_{p,CO} T_g \frac{M_{CO}}{M_C}\frac{d[\text{pct C}]}{dt} \\
&\quad - \left(\Delta H_C \frac{d[\text{pct C}]}{dt} + \Delta H_{Cr}\frac{d[\text{pct Cr}]}{dt} + \Delta H_{Mn}\frac{d[\text{pct Mn}]}{dt}\right. \\
&\quad \left.\left. + \Delta H_{Si}\frac{d[\text{pct Si}]}{dt}\right)\right)/(100\, c_{p,m} + 100\, c_{p,s} W_s / W_m)
\end{aligned}
$$

where $q_{loss} = q_1 + q_2 + q_3 + q_4 + q_u$. In the present work, the refractory lining with the shell was referred to approximately as a multilayer plate; q_1, q_2, q_3, and q_4 were, respectively, determined in terms of the one-dimensional transient heat-conduction problems; q_5 was taken to be $\frac{W_1 C_{p,1}}{\Delta T}$ and $q_u = (q_1 + q_2 + q_3 + q_4) \times 15$ pct.

It should be pointed out that Eq. [22] included not only the influence of the changes in the amounts of molten steel and slag, but also the heat needed for the rise of the refractory-lining temperature during the refining process. The initial and boundary conditions of the model involve the initial amounts, chemical composition, and temperature of the molten steel and slag; the blowing rates and temperatures of the oxygen and inert gas (argon or nitrogen); the temperatures of the shell and exhaust gas; the amounts of various addition agents.

IV. DETERMINATION AND ESTIMATION OF PARAMETERS FOR THE MODEL

A. *Distribution Ratios of Blown Oxygen among Elements*

This is a very important parameter for the model. It has been either treated using different ways or simply evaded in the literature, and it has not been reasonably determined until now. Tohge *et al.*[8] have used the free energy of each oxide and the concentration difference of each element to determine the parameter. Relatively, that is more reasonable, but the concentration difference has to be determined. It may be believed that the distribution ratios of the blown oxygen among the elements dissolved in the steel would be proportional to the Gibbs free energies of their oxidation reactions at the interface. From this consideration, the following relationships should be held:

$$x_C = \frac{\Delta G_C}{\Delta G_C + \Delta G_{Cr}/3 + \Delta G_{Mn} + \Delta G_{Si}/2} \qquad [23]$$

$$x_{Cr} = \frac{\Delta G_{Cr}/3}{\Delta G_C + \Delta G_{Cr}/3 + \Delta G_{Mn} + \Delta G_{Si}/2} \qquad [24]$$

$$x_{Si} = \frac{\Delta G_{Si}/2}{\Delta G_C + \Delta G_{Cr}/3 + \Delta G_{Mn} + \Delta G_{Si}/2} \qquad [25]$$

$$x_{Mn} = \frac{\Delta G_{Mn}}{\Delta G_C + \Delta G_{Cr}/3 + \Delta G_{Mn} + \Delta G_{Si}/2} \qquad [26]$$

B. *Activity Coefficients*

The activity coefficients of the components in the molten steel can be estimated using the interaction parameters $e_i^{(j)}$. The values of $e_i^{(j)}$ were all taken from Reference 19 in the present work (Table I).

There is no CaF_2 in the slag, and the temperature was lower at the early stage of the refining. Based on the expressions of the activity coefficients of the components in the molten slag used for electroslag remelting of stainless steel,[18] Eqs. [27a] through [30a] were employed to calculate the activity coefficients of the oxide components in the slag for the early period of the refining.

$$
\begin{aligned}
\lg \gamma_{FeO} &= \frac{3540}{T}(N_{CaO} + N_{MgO})(N_{SiO_2} + 0.25\, N_{AlO_{1.5}}) \\
&\quad + \frac{1475}{T} N_{MnO}(N_{SiO_2} + 0.45\, N_{CrO_{1.5}}) \qquad [27a] \\
&\quad + \frac{1068}{T} N_{AlO_{1.5}} N_{SiO_2} + \frac{36}{T} N_{MnO} N_{AlO_{1.5}} \\
&\quad + \frac{593}{T} N_{CrO_{1.5}} N_{SiO_2}
\end{aligned}
$$

Table I. Interaction Coefficients $e_i^{(j)}$ used in the present work[19]

	The third element j						
Element i	C	Cr	Mn	Si	O	Ni	Mo
C	0.14	−0.024	−0.012	0.08	−0.34	0.012	−0.0083
Cr	−0.12	−0.0003	—	−0.0043	−0.14	0.0002	0.0018
Mn	−0.0538	0.0039	—	—	−0.083	—	—
Si	0.24	0.015	0.002	0.37	—	0.005	—

$$\lg \gamma_{FeO} = \frac{4130}{T}(N_{CaO} + N_{MgO})(N_{SiO_2} + 0.25\, N_{AlO_{1.5}}) + \frac{1720}{T} N_{MnO}(N_{SiO_2} + 0.45\, N_{CrO_{1.5}}) + \frac{1246}{T} N_{AlO_{1.5}} N_{SiO_2} + \frac{42}{T} N_{MnO} N_{AlO_{1.5}} + \frac{692}{T} N_{CrO_{1.5}} N_{SiO_2} \quad [27b]$$

$$\lg \gamma_{Cr_2O_3} = \lg \gamma_{FeO} - \frac{1594}{T}(N_{CaO} + N_{MgO}) - \frac{664}{T} N_{MnO} - \frac{593}{T} N_{SiO_2} \quad [28a]$$

$$\lg \gamma_{Cr_2O_3} = \lg \gamma_{FeO} - \frac{1859}{T}(N_{CaO} + N_{MgO}) - \frac{774}{T} N_{MnO} - \frac{692}{T} N_{SiO_2} \quad [28b]$$

$$\lg \gamma_{SiO_2} = \lg \gamma_{FeO} - \frac{3540}{T}(N_{CaO} + N_{MgO}) - \frac{1475}{T} N_{MnO} - \frac{1068}{T} N_{AlO_{1.5}} - \frac{593}{T} N_{CrO_{1.5}} \quad [29a]$$

$$\lg \gamma_{SiO_2} = \lg \gamma_{FeO} - \frac{4130}{T}(N_{CaO} + N_{MgO}) - \frac{1720}{T} N_{MnO} - \frac{1246}{T} N_{AlO_{1.5}} - \frac{692}{T} N_{CrO_{1.5}} \quad [29b]$$

$$\lg \gamma_{MnO} = \lg \gamma_{FeO} - \frac{1475}{T}(N_{SiO_2} + 0.45\, N_{CrO_{1.5}}) - \frac{36}{T} N_{AlO_{1.5}} \quad [30a]$$

$$\lg \gamma_{MnO} = \lg \gamma_{FeO} - \frac{1720}{T}(N_{SiO_2} + 0.45\, N_{CrO_{1.5}}) - \frac{42}{T} N_{AlO_{1.5}} \quad [30b]$$

For the latter period of the refining, at which the bath temperature has been evidently heightened, Eqs. [27b] through [30b] were taken in this work. Also, the solubility of Cr_2O_3 in the slag is about 5 mass pct.[20] Consequently, $a_{Cr_2O_3}$ was taken to be 1 if $(Cr_2O_3) \geq 5$ mass pct in the present work.

C. *Equilibrium Constants of Reactions*

For reaction [6], from

$$[C] + [O] = \{CO\}, \qquad \lg K_{C\text{-}O} = 2525/T + 1.43^{[21]}$$

$$[Fe] + [O] = (FeO), \qquad \lg K_{Fe\text{-}O} = 6320/T - 2.734^{[22]}$$

it can be obtained that

$$\lg K_c = -3795/T + 4.164 \quad [31]$$

For reactions [7] through [9] and [15], the equilibrium constants were taken, respectively, as

$$\lg K_{Cr} = 24{,}025/T - 10.566^{[18]} \quad [32]$$

$$\lg K_{Si} = 17{,}770/T - 6.122^{[16]} \quad [33]$$

$$\lg K_{Mn} = 8695/T - 3.93^{[16]} \quad [34]$$

$$\lg K_{Cr\text{-}C} = 35{,}410/T - 23.058 \quad [35]$$

D. *Mass-Transfer Coefficient of Carbon in Liquid Steel*

The following expression was used to calculate the mass-transfer coefficient of carbon in the liquid steel (k_C):[23]

$$k_C = 0.8\, r_{eq}^{-1/4}\, D_C^{1/2} g^{1/4} \quad [36]$$

At a sufficiently high velocity of gas stream, each bubble in the bubble group roughly has a uniform size.[24] On the basis of the results of water modeling in a prior work,[13] the average diameter of a bubble (d_b) was taken to be 2.5 cm, with $D_C = 7.46$ cm^2/s.[5]

E. *Estimation of the Area of Reaction Interface*

During the AOD refining process, the oxidative or reductive reactions of elements will occur at the bubble surface. Therefore, the area of the reaction interface (A_{rea}) will be approximately the total surface area of the bubbles. Using the expression for estimating the total number of bubbles, given by Diaz *et al.*[25] as $n_b = 6\, QH_b/(\pi d_b^3\, u_b)$, the following can be obtained:

$$A_{rea} = 6\, QH_b/(d_b u_b) \quad [37]$$

where $H_b = 95$ cm for an 18-t AOD vessel and u_b can be found from Eq. [38]:[26]

$$u_b = 1.02\, (g d_b/2)^{1/2} \quad [38]$$

F. *Oxidation Enthalpies of Elements*

The oxidation enthalpies of the elements in the steel were estimated in terms of the direct oxidation reactions by the blown oxygen. The standard enthalpies at (298 K) of the

Table II. Change in Temperature Caused by Added 1 kg Alloy for 1 t Molten Steel, K[29]

Alloy	High carbon Fe-Cr	Middle carbon Fe-Cr	Low carbon Fe-Cr	Middle carbon Fe-Mn	High carbon Fe-Mn	Electrolitic Mn	Metallic Ni	Mn-Si	75 Si-Fe
ΔT, K	−2.3	−2.0	−1.8	−2.01	−2.26	−1.98	−1.39	−1.58	+0.57

respective oxide formation involved in the following equations were all taken from Reference 27, and the relevant heat capacities at constant pressure with the enthalpies of solution formation were taken from Reference 28.

$$\Delta H_C = \Delta H_{CO} - \Delta H_{[C]} - 1/2\ \Delta H_O = 11{,}852 - (2.367\ T_g + 1.708 \times 10^{-4} T_g^2 + 3.835 \times 10^3/T_g) \quad [39]$$

$$\Delta H_C = \Delta H_{Cr_2O_3} - 2\Delta H_{[Cr]} - 3/2\ \Delta H_O = 11{,}519 - (1.148T + 4.4 \times 10^{-5}\ T^2 + 1.5 \times 10^4/T) \quad [40]$$

$$\Delta H_{Si} = \Delta H_{SiO_2} - \Delta H_{[Si]} - \Delta H_O = 30{,}658 - (2.15\ T + 1.45 \times 10^{-4} T^2) \quad [41]$$

$$\Delta H_{Mn} = \Delta H_{MnO} - \Delta H_{[Mn]} - 1/2\ \Delta H_O = 7581 - (0.845\ T + 7.38 \times 10^{-5}\ T^2 + 6.69 \times 10^4/T) \quad [42]$$

The other physical constants were, respectively, taken to be $\rho_m = 7.37$ g/cm^3,[18] $\rho_s = 3.1$, $\rho_{O_2} = 1.4277 \times 10^{-3}$, $\rho_{Ar} = 1.7821 \times 10^{-3}$, $\rho_{N_2} = 1.2499 \times 10^{-3}$ g/cm^3, $c_{p,m} = 0.8159$, $c_{p,s} = 1.1966$, $c_{p,scrap} = 0.7113$, $c_{p,O_2} = 0.9184$, $c_{p,Ar} = 0.5238$, $c_{p,N_2} = 1.0376$, $c_{p,CO} = 1.0447$, and $c_{p,CaO} = 0.9205$ J·g-1·K^{-1}, from Reference 28. The thermal conductivities of the various refractory materials and shell (steel plate) were $\lambda_{Mg\text{-}Cr} = 0.0198$, $\lambda_{Mg\text{-}Al} = 0.0233$, $\lambda_{cl} = 0.0177$, $\lambda_{as} = 0.0016$, $\lambda_{mag} = 0.0243$, and $\lambda_{sh} = 0.50$ W·cm^{-1}·K^{-1}, also from Reference 28.

G. *Estimation of the Cooling Effects of Addition Agents*

The temperature drop caused by added alloy agents is

$$\Delta T = z_{alloy} W_{alloy} \times 10^{-3}/(W_m \times 10^{-6}) \quad [43]$$

where z_{alloy} is the chill factor, in K·kg^{-1}. The values of the factor for some alloys are shown in Table II.[29]

The temperature drop caused by added lime is

$$\Delta T = W_{CaO}(Q_{ph} - Q_{ch})/(W_m c_m + W_s c_s) \quad [44]$$

Here, $Q_{ph} = c_{p,CaO}(T - T_{CaO}) + Q_{melt,CaO}$, $Q_{melt,CaO} \approx 1419.46$ J·g^{-1},[30] and $Q_{ch} \approx 1280.23$ J·g^{-1}.[31]

The following equation was used to estimate the temperature drop caused by added crop ends and scrap:

$$\Delta T = \frac{(T_{melt} - T_{scrap})c_{p,scrap} + Q_{melt,m} + (T - T_{melt})c_{p,m}}{W_m c_{p,m} + W_s c_{p,s}} \quad [45]$$

where $Q_{melt,m} \approx 251$ J·g^{-1};[28] the melting point of the steel (T_{melt}) can be determined by the following expression:[32]

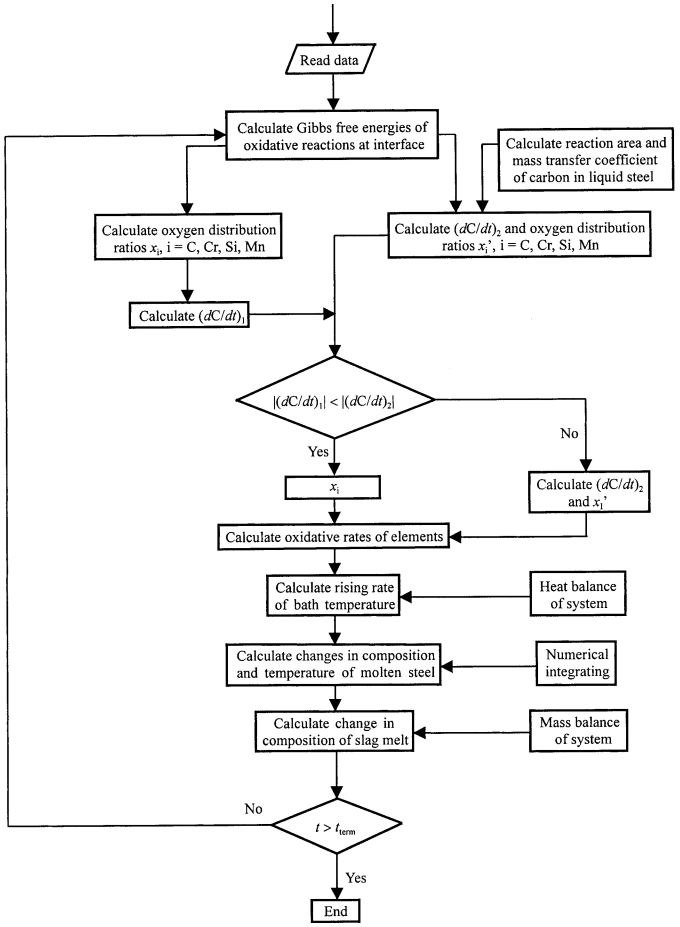

Fig. 1—Flow chart for computer program.

$$T_{melt} = 1538 - 65[\text{pct C}] - 30[\text{pct P}] - 25[\text{pct S}] - 20[\text{pct Ti}] - 8[\text{pct Si}] - 7[\text{pct Cu}] - 5[\text{pct Mn}] - 4[\text{pct Ni}] - 3[\text{pct Al}] - 2[\text{pct V}] - 2[\text{pct Mo}] - 1.5[\text{pct Cr}] - 1.5[\text{pct Co}] - [\text{pct W}] \quad [46]$$

V. NUMERICAL SOLUTION FOR THE MODEL

The model can be used to deal with the AOD refining process of stainless steel, including the first and second blowing periods (also the third period, for the ultralow-carbon steel). The flow chart for the computer program is presented in Figure 1.

It can be seen from Figure 1 that, first, the appropriate distribution ratios of blown oxygen are determined from the obtained Gibbs free energies of the oxidative reactions of elements. Further, the decarburization rate related to the oxygen flow rate (dC_1/dt) is calculated; on the other hand, the decarburization rate controlled by the mass transfer of

carbon in the molten steel (dC_2/dt) is also calculated. Comparing these two rates, if $|dC_1/dt| < |dC_2/dt|$, the rising rate of the bath temperature is computed with $|dC_1/dt|$, the oxidation rates of the other elements, and the corresponding oxidative enthalpies. Otherwise, the relevant amount of oxygen consumption to carbon is achieved using $|dC_2/dt|$, and the oxidation rates of chromium, silicon, and manganese are found using the surplus oxygen amount and the oxygen distribution ratios obtained from the Gibbs free energies of their oxidation reactions. Then, the appropriate rising rate of the bath temperature is also calculated. Finally, the concentrations of the components in the steel and the bath temperature can be obtained by numerical integrating, and the concentrations of the components in the slag melt can be determined from the mass balance of the system. The effect of FeO on the mass and heat balances can be neglected, because it is referred to as an intermediate product of the gas-blowing refining. The ultimate output results are the changes in the chemical composition, temperature and amount of the liquid steel and slag melt, the distribution ratios of oxygen among the elements, the decarburization rate with the blowing refining time.

The model has been used to deal with and analyze the austenitic stainless steel making (including ultralow carbon steel) in an 18-t AOD vessel and tested on data of 32 heats obtained in producing 18Cr9Ni grade steel. The application of the model to the AOD industrial practice and the results will be reported in Part 2 of the present work.

LIST OF SYMBOLES

A_{rea}	total reaction interface, cm^2
a_{i}	activity of i component
$c_{p,\text{i}}$	specific heat of i substance at constant pressure, $J \cdot g^{-1} \cdot K^{-1}$
D_C	diffusion coefficient of carbon in molten steel, $cm^2 \cdot s^{-1}$
d_b	average diameter of bubble, cm
f_{i}	Henrian activity coefficient of component i in molten steel
ΔG_{i}	Gibbs free energy for oxidation reaction of i element, $J \cdot g^{-1}$
g	acceleration due to gravity, $cm \cdot s^{-2}$
H_b	rising height of bubble, cm
ΔH_{i}	oxidation enthalpy of i element, $J \cdot g^{-1}$
[pct i]	mass percent concentration of i solute in molten steel, mass pct
$[\text{pct i}]_e$	equilibrium concentration of i solute in molten steel at reaction interface, mass pct
(pct j)	mass percent concentration of j component in slag melt, mass pct
K_{i}	equilibrium constant for indirect oxidation reaction of i solute in molten steel
$K_{\text{Cr-C}}$	equilibrium constant of $[C](Cr_2O_3)$ reaction
k_{C}	mass transfer of carbon in molten steel, $cm \cdot s^{-1}$
M_{i}	mole mass of i substance, $g \cdot mole^{-1}$
N_{j}	mole fraction concentration of j component in slag
n_b	total number of bubble
n_i	mole flow rate of i component, $mole \cdot s^{-1}$
P_{CO}	partial dimensionless pressure of carbon monoxide
P_t	total dimensionless pressure in AOD vessel
p_t	average absolute pressure in AOD vessel, atm
Q	total gas flow rate, $cm^3 \cdot s^{-1}$
Q_{ph}	physical heat of lime melting and dissolving in molten slag, $J \cdot g^{-1}$
Q_{ch}	chemical heat of lime dissolving in slag melt, $J \cdot g^{-1}$
Q_i	flow rate of i gas, $cm^3 \cdot s^{-1}$
Q_{sub}	total flow rate of inert gas, $cm^3 \cdot s^{-1}$
q_1	heat loss by conduction from bottom of the vessel, $J \cdot s^{-1}$
q_2	heat loss by conduction from the lower of the vessel, $J \cdot s^{-1}$
q_3	heat loss by conduction from the upper of the vessel, $J \cdot s^{-1}$
q_4	heat loss by conduction from top of the vessel, $J \cdot s^{-1}$
q_5	heat loss absorbed by refractory lining of the vessel during bath rising temperature, $J \cdot s^{-1}$
q_u	uncertain heat loss of the system, $J \cdot s^{-1}$
R	gas constant (=8.314), $J \cdot mol^{-1} \cdot K^{-1}$
r_b	mean radius of bubble, cm
r_{eq}	mean equivalent radius of bubble, cm
T	bath temperature, K
T_g, T_{g0}	temperature of gas and its initial value, K
u_b	velocity of bubble, $cm \cdot s^{-1}$
W_{alloy}	mass of alloy agents added, g
W_{CaO}	mass of lime added, g
W_m	mass of liquid steel, g
W_s	mass of slag, g
x	distribution ratio of oxygen for i component in liquid steel
γ	Raoultian activity coefficient of j component in slag melt
η	utilization ratio of oxygen
λ	heat conductivity of i material, $W \cdot cm^{-1} \cdot K^{-1}$
ρ	density of i material, $g \cdot cm^{-3}$

Subscripts

as	asbestos board
cl	clay brick
Mg-Al	alumina-magnesite brick
Mg-Cr	chrome-magnesite brick
Mag	magnesite
m, s, l	metal, slag phase and lining, respectively
sh	shell

[ ]—metal phase; ( )—slag phase; { }—gaseous phase; and ⟨ ⟩—solid phase

ACKNOWLEDGMENTS

The authors gratefully acknowledge the support of the National Natural Science Foundation of China (Grant No. 5947016). The Shanghai No. 5 Iron and Steel (Group) Corporation kindly offered the data on AOD heats.

REFERENCES

1. W.H. Ray and J. Szekely: *Process Optimization with Applications in Metallurgy and Chemical Engineering*, John Wiley & Sons, Interscience, New York, NY, 1971, pp. 310-19.
2. S. Asai and J. Szekely: *Metall. Trans*, 1974, vol. 5, pp. 651-57.
3. J. Szekely and S. Asai: *Metall. Trans*, 1974, vol. 5, pp. 1573-80.

4. R.J. Fruehan: *Ironmaking and Steelmaking*, 1976, vol. 3, pp. 153-58.
5. T. Deb Roy and D.G.C. Robertson: *Ironmaking and Steelmaking*, 1978, vol. 5(5), pp. 198-206.
6. T. Deb Roy and D.G.C. Robertson: *Ironmaking and Steelmaking*, 1978, vol. 5(5), pp. 207-10.
7. T. Ohno and T. Nishida: *Tetsu-to Hagané*, vol. 63(13), pp. 2094-99.
8. T. Tohge, Y. Fujita, and T. Watanabe: *Proc. 4th Process Technology Conf.*, Iron & Steel Society, Chicago, IL, 1984, pp. 129-36.
9. J. Reichel and J. Szekely: *Iron Steelmaker*, 1995, No. 5, pp. 41-48.
10. M. Görnerup and P. Sjöberg: *Ironmaking and Steelmaking*, 1999, vol. 26(1), pp. 58-63.
11. D.A. Lewis, D.E. Pauley, C.E. Rea, M.E. Shupay, and J.D. Nauman: *Proc. Annual Convention of 1998 AISE (CD edition)*, Pittsburgh, PA, Sept. 23–25, 1998.
12. H. Gorges, W. Pulvemacher, W. Rubens, and H. Diersten: *Proc. 3rd Int. Iron Steel Congr.*, Chicago, IL, Apr. 16–20, 1978, pp. 161-67.
13. Ji-He Wei, Jin-Chang Ma, Yan-Yi Fan, Neng-Wen Yu, Sen-Long Yang, Shun-Hua Xiang, and De-Ping Zhu: *Ironmaking and Steelmaking*, 1999, vol. 26(5), pp. 363-71.
14. Wei Chi-ho (Ji-He Wei) and A. Mitchell: *Proc. 3rd Process Technology Conf.*, Mar. 28–31, 1982, ISS, Pittsburgh, PA, vol. 3, pp. 232-54.
15. A. Mitchell, F.R. Carmona, and Wei Chi-ho (Ji-He Wei): *Iron Steelmaker*, 1982, No. 3, pp. 37-41.
16. Wei Jihe (Ji-He Wei) and A. Mitchell: *Chin. J. Met. Sci. Technol.*, 1986, vol. 2(1), pp. 11-31.
17. Wei Jihe (Ji-He Wei) and A. Mitchell: *Acta Metall. Sinica*, 1987, vol. 23(3), pp. B126-B134.
18. Wei Jihe (Ji-He Wei): *Chin. J. Met. Sci. Technol.*, 1989, vol. 5(4), pp. 235-46.
19. G.K. Sigworth and J.F. Elliott: *Met. Sci.*, 1974, vol. 8, pp. 298-310.
20. E.T. Turkdogan: *Physicochemical Properties of Molten Slags and Glasses*, Metals Society, London, 1983, p. 422.
21. V.T. Burtsev, V.G. Glebovskii, V.I. Kashin, and L.N. Sakosnova: *Deoxidation Power of Carbon in Molten Iron, Cobalt and Nickel, Izv. AN USSR, Metals*, 1974, No. 1, pp. 3-8.
22. J. Chipman: *Basic Open Hearth Steelmaking*, 3rd ed., G. Derge, ed., AIME, Warrendale, PA, 1964, p. 531.
23. M.H.I. Baird and J.F. Davidson: *Chem. Eng. Sci.*, 1962, vol. 17, pp. 87-93.
24. E.T. Turkdogan: *Physical Chemistry of High Temperature Technology*, Academic Press, New York, NY, 1980, p. 359.
25. M.C. Diaz, S.V. Komarov, and M. Sano: *Iron Steel Inst. Jpn. Int.*, 1997, vol. 37(1), pp. 1-8.
26. R.M. Davice and G.I. Taylor: *Proc. R. Soc. London*, 1950, Ser. A200, p. 375.
27. E.T. Turkdogan: *Physical Chemistry of High Temperature Technology*, Academic Press, New York, NY, 1980, pp. 5-69.
28. Jia-Xiang Chen: *Handbook of Common Using Data, Graphs and Tables in Steelmaking*, Metallurgical Industry Press, Beijing, 1984, ch. 1.
29. *The Making, Shaping and Treating of Steel*, 10th ed., by W.T. Lankford, Jr., N.L. Samways, R.F. Craven, and H.E. McGannon, eds., American Steel Corporation, Ohio, 1985, p. 368.
30. E.T. Turkdogan: *Physical Chemistry of High Temperature Technology*, Academic Press, New York, NY, 1980, p. 14.
31. H.A. Fine and G.H. Geiger: *Handbook on Material and Energy Balance Calculations in Metallurgical Processes*, AIME, Warrendale, PA, 1979, p. 106.
32. Jia-Xiang Chen: *Handbook on Common Using Data, Graphs and Tables in Steelmaking*, Metallurgical Industry Press, Beijing, 1984, p. 383.